The tetravalent, bispecific properties of FS118, an anti-LAG-3/PD-L1 antibody, mediate LAG-3 shedding from CD4+ and CD8+ tumor-infiltrating lymphocytes

Claire S. Reader[a], Wenjia Liao[b], Beatrice J. Potter-Landua[a], Christel Séguy Veyssier[a], Claire J. Seal[a], Neil Brewis[b] and Michelle Morrow[a]

Tumor-infiltrating lymphocytes (TILs) often have upregulated expression of immune checkpoint receptors, such as programmed cell death 1 (PD-1) and lymphocyte-activation gene 3 (LAG-3). Patients treated with antibodies targeting PD-1 or its ligand (PD-L1) can develop resistance or relapse, with LAG-3 upregulation on T cells being one possible mechanism. FS118 is a tetravalent, bispecific antibody comprising a full-length IgG_1 anti-PD-L1 antibody with bivalent LAG-3-binding capability in the fragment crystallizable region. Here we demonstrate how the structure of FS118 is important for its function. We generated variants of FS118 and tested their ability to mediate LAG-3 shedding using staphylococcal enterotoxin B assays, antigen recall assays, and soluble LAG-3 ELISAs. Mediated by metalloproteases ADAM10 and ADAM17, FS118 induced shedding of LAG-3 from the surface of both CD4+ and CD8+ T cells. We also determined the effect of surrogate antibodies on immune cell LAG-3 expression and proliferation in syngeneic mouse models. *In vivo*, the bivalent LAG-3 binding sites of a mouse surrogate of FS118 and their location in the fragment crystallizable region were important for eliciting maximal reduction in LAG-3 levels on the surface of TILs, as variants with a single LAG-3 binding site in the fragment crystallizable region, or with reversed orientation of the LAG-3 and PD-L1 binding sites, were less efficient at inducing shedding. We also show that PD-L1, not PD-1, binding drives the LAG-3 reduction on TILs. We hypothesize that the LAG-3 bivalency in the fragment crystallizable region of FS118 allows LAG-3 clustering, which optimizes cleavage by ADAM10/ADAM17 and thus shedding. *Anti-Cancer Drugs* 36: 447–458 Copyright © 2025 The Author(s). Published by Wolters Kluwer Health, Inc.

Anti-Cancer Drugs 2025, **36**:447–458

Keywords: bispecific antibody, FS118, immunotherapy, lymphocyte-activation gene 3, programmed death ligand 1, tetravalent

[a]invoX Pharma and [b]F-star Therapeutics, Cambridge, UK

Correspondence to Neil Brewis, PhD, F-star Therapeutics Ltd, Babraham Research Campus, Cambridge CB22 3AT, UK
Tel: +44 1223 497400; e-mail: neil.brewis@f-star.com

Received 26 November 2024 **Revised form accepted** 6 December 2024.

Introduction

An immunosuppressive environment can develop within tumors, leading to exhaustion of tumor-infiltrating lymphocytes (TILs), typified by changes such as reduced proliferation and increased expression of immune checkpoint receptors [1]. Among these receptors are programmed cell death 1 (PD-1) and lymphocyte-activation gene 3 (LAG-3) [2], both of which are involved in maintaining immune tolerance [3,4].

PD-1 limits T-cell activity by binding to ligands, including programmed death ligand 1 (PD-L1), on the surface of certain immune cells, preventing autoimmunity, and on tumor cells, preventing tumor destruction [3,5]. A number of PD-(L)1-targeting antibodies are now approved for the treatment of certain cancers [6]. However, when used as monotherapy, only a limited number of patients respond to these agents, and some responders later relapse [7,8]. One possible mechanism of resistance to PD-(L)1-targeting antibodies is compensatory upregulation of LAG-3 and other checkpoint proteins [9,10].

LAG-3 is expressed on various immune cells, including activated T cells [11,12]. It is structurally homologous to the CD4 T cell co-receptor and can suppress effector T-cell activity via binding to major histocompatibility complex (MHC) class II-peptide complexes [13,14]. Several anti-LAG-3 antibodies are currently in clinical development, either as monotherapy or in combination with other immune checkpoint inhibitors [15]. One such combination, the anti-LAG-3 mAb relatlimab and the anti-PD-1 mAb nivolumab, has been approved for the treatment of advanced melanoma in the USA [16] and European Union (EU) [17], based on a Phase II/III trial that demonstrated a progression-free survival benefit with the combination vs nivolumab alone [18]. Other similar combinations include fianlimab (anti-LAG-3 mAb) plus

Supplemental Digital Content is available for this article. Direct URL citations appear in the printed text and are provided in the HTML and PDF versions of this article on the journal's website, www.anti-cancerdrugs.com.

cemiplimab (anti-PD-1 mAb), which has shown a promising benefit–risk profile in patients with advanced melanoma in a Phase I trial [19], and ieramilimab (anti-LAG-3 mAb) plus spartalizumab (anti-PD-1 mAb), which has demonstrated durable efficacy in some patients with various advanced solid malignancies in a Phase II trial [20]. Another method of LAG-3/PD-(L)1 dual blockade under investigation is the use of bispecific monoclonal antibodies that target both proteins. Several such antibodies are under clinical investigation [15], including FS118 [21].

FS118 is a human tetravalent bispecific mAb (mAb^2), comprising a full-length IgG_1 PD-L1 mAb with distinct LAG-3-binding capability introduced into the fragment crystallizable region [defined as an fragment crystallizable region with antigen binding (Fcab)] [22,23]. Additional mutations were engineered into the CH2 domain [leucine-alanine amino acid substitutions (LALA) at positions 1.3 and 1.2 (IMGT numbering)] to decrease Fcγ receptor binding and therefore reduce antibody-dependent cell-mediated cytotoxicity [24].

We have previously shown that FS118 blocks LAG-3 and PD-L1 inhibitory signaling to overcome immunosuppressive signals, with comparable or better activity than the combination of the individual components [23]. In syngeneic tumor mouse models, a mouse surrogate FS118 bispecific antibody (FS118m; previously referred to as mLAG-3/PD-L1 mAb^2) demonstrated superior tumor growth inhibition to that observed with anti-LAG-3 or anti-PD-L1 antibodies used individually and in combination [23]. Furthermore, FS118m induced shedding of LAG-3 from the surface of TILs, with a corresponding increase in soluble LAG-3 (sLAG-3) in the serum [23]. Similarly, in a Phase I trial (NCT03440437), FS118 was associated with a dose-dependent increase in sLAG-3 in the serum of patients with advanced malignancies [21].

A recent study suggests that LAG-3 shedding, mediated by metalloprotease domain-containing proteins (ADAM10 and ADAM17), is essential for overcoming resistance to anti-PD-1 immunotherapy [25]. Here we generated a series of FS118 and FS118m variants to investigate how certain features of the FS118 structure may be involved in the induction of LAG-3 shedding from TILs. We found that the tetravalent structure of FS118 was required to achieve the highest levels of LAG-3 shedding. This study demonstrates how the design and structure of a bispecific antibody can lead to unique biological function.

Materials and methods

Antibody generation and nomenclature

FS118 and the mouse surrogate FS118m (also known as mLAG-3/PD-L1 mAb^2) were constructed as previously described [23]. For the valency variant of FS118 with monovalent LAG-3 binding (LAG-3_1/PD-$L1_2$ mAb^2), the monovalent LAG-3-targeting region comprised a human LAG-3 Fcab domain paired with a wild-type human IgG_1 CH3 domain using knobs-into-holes mutations [26]. The mouse surrogate of the monovalent LAG-3-binding antibody, mLAG-3_1/PD-$L1_2$ mAb^2, was constructed by introducing a LAG-3 binding site into a CH3 domain of a mouse IgG_1 mAb with PD-L1-binding fragment antigen binding (Fab) domains (sequence from clone YW243.55.S1, Genentech patent publication US20100203056A1; 'mPD-L1 mAb'). The variant of FS118m in which the PD-L1 binding sites were replaced with PD-1 binding sites (mLAG-3/PD-1 mAb^2) was constructed by introducing a LAG-3 binding site into each of the CH3 domains of a mouse IgG_1 mAb with PD-1-binding Fab domains (sequence from clone RMP1-14; the anti-mouse PD-1 hybridoma cell line was provided by Dr. Hideo Yagita from Juntendo University School of Medicine). The antibody in which the positions of the PD-L1 and LAG-3 binding sites of FS118m were reversed (mPD-L1/LAG-3 mAb^2; also referred to as the reverse orientation antibody) was constructed by introducing a PD-L1 binding site into each of the CH3 domains of a mouse IgG_1 mAb with LAG-3-binding Fab domains (sequence from clone C9B7W; the hybridoma cell line was provided by St. Jude Children's Research Hospital). Where indicated, LALA mutations [27] were implemented via site-directed mutagenesis.

All mAb or mAb^2 sequences were incorporated into pTT5 expression vectors (National Research Council of Canada, Ottawa, Ontario, Canada). Transfection of vectors into Expi293F cells [Thermo Fisher Scientific, Loughborough, UK; A14528 (RRID: CVCL_D615)] was undertaken using a PEIpro Transfection Reagent (PPLU115; Polyplus, Graffenstaden, France) protocol adapted from the manufacturer's instructions. Expression of sufficient heterodimeric knobs-into-holes-containing antibodies required iterative optimization of HC1 : HC2 : LC DNA ratios during transfection [26]. Cell cultures were harvested using centrifugation, or with a diatomaceous earth (SDLKG-10.0; Sartoclear, Epsom, UK), and filtration. Clarified supernatants were purified using 5 ml MabSelect SuRe columns (11003494; Cytiva, Little Chalfont, UK) on an AKTA system (Cytiva; Xpress, Pure, Avant, or Explorer) using a protocol adapted from the manufacturer's instructions. Further purification was achieved using HiLoad 26/600 Superdex 200 pg columns (28989336; Cytiva), which also separate heterodimeric antibodies that differ in size from homodimeric parent molecule contaminants. Where heterodimeric antibodies were of highly similar size to homodimeric parent molecule contaminants, additional separation was achieved with HiTrap Capto Butyl ImpRes columns (17371912; Cytiva) using a protocol adapted from the manufacturer's instructions.

Crosslinking mass spectrometry

Crosslinking mass spectrometry (XL/MS) mapping by high-mass matrix-assisted laser desorption/ionization (MALDI) MS was used to directly analyze non-covalent interactions between FS118 and target proteins (LAG-3 and PD-L1) with high sensitivity [28]. Prior to mixing FS118, LAG-3, and PD-L1, control samples of each protein were analyzed by high-mass MALDI MS at concentrations representative of the mixing experiments, to verify their integrity and aggregation level. PD-L1 and LAG-3 were dissolved in distilled water to 200 mg/ml; FS118 solution was 4 mg/ml. From each solution, a 1 to 1/128 dilution series was prepared.

For control experiments, 1 µl of each dilution was mixed with 1 µl of a matrix composed of recrystallized sinapinic acid. After mixing, 1 µl of each sample was spotted on the MALDI plate. After crystallization at room temperature (RT), the plate was analyzed in the MALDI mass spectrometer in high-mass MALDI mode. Analyses were repeated in triplicate.

For crosslinking experiments, lysine-based BS3 crosslinkers (CovalX, Bordeaux, France) were used to stabilize complexes that were amenable to high-mass MALDI-MS analysis. Binding reactions were set up based on the molar concentrations of each species in the final volume; reactions used either equal amounts of FS118 to LAG-3 and PD-L1 [concentrations of FS118, LAG-3, and PD-L1 were 1 µM, 2 µM, and 2 µM, respectively (1 : 2 : 2 ratio)] or excess PD-L1 [concentrations of FS118, LAG-3, and PD-L1 were 1 µM, 2 µM, and 10 µM, respectively (1 : 2 : 10 ratio)]. K200 Stabilizer reagent (1 µl; 2 mg/ml) from the K200 MALDI MS analysis kit (CovalX) was mixed with 9 µl of each reaction mixture. Samples were incubated at RT for 180 min, prepared for MALDI analysis as for control experiments, and analyzed by high-mass MALDI after crystallization.

MALDI time-of-flight MS analysis, with an HM4 interaction module (CovalX) and a standard nitrogen laser, was performed, focusing on masses of 0–1500 kDa. The following mass spectrometer parameters were applied: linear and positive mode; ion source 1, 20 kV; ion source 2, 17 kV; lens, 12 kV; pulse ion extraction, 400 ns; HM4 gain voltage, 3.14 kV; and HM4 acceleration voltage, 20 kV. Spectra peak intensity was used to estimate the relative amount of protein and complexes present.

In-vitro T-cell functional assays

Staphylococcal enterotoxin B assay

Human peripheral blood mononuclear cells (PBMCs) were isolated from whole blood using Ficoll-Paque density gradient centrifugation (17-5446-02; GE Healthcare, Little Chalfont, UK). $CD4^+$ T cells and monocytes were isolated using negative selection (130-0560533, 130-096-537; Miltenyi Biotec, Bisley, UK). $CD4^+$ T cells were expanded for 8 days using anti-CD3/CD28 dynabeads (1131D; Thermo Fisher Scientific), and monocytes were cultured in Mo-DC differentiation medium (130-094-812; Miltenyi Biotec) and differentiated into immature dendritic cells (iDC) for 7 days; 1×10^5 expanded $CD4^+$ T cells and 1×10^4 iDC were cocultured and stimulated with Staphylococcal enterotoxin B (SEB) (S4881; Sigma, Glasgow, UK) for 4 days in the presence of various concentrations of test antibodies, with or without inhibitors of ADAM10 (GI254023X, Tocris, Abingdon, UK, 3995) [29] or ADAM17 (TAPI-1, Tocris, 6162) [30]. Cell culture supernatants were harvested, and sLAG-3 levels were quantified by ELISA.

Antigen recall assay

Human PBMCs were activated by MHC class II-restricted CEF (PX-CEF-G; ProImmune, Oxford, UK) or MHC class I restricted CEFT peptide pools (PX-CEFT-G; ProImmune) in cell culture medium containing 1 ng/ml IL-2 (200-02; PeproTech, Paisley, UK) and 5 ng/ml IL-7 (200-07; PeproTech) for 7 days. Cells were refed with IL-2 and IL-7 after 3 days incubation. After 7 days incubation, cells were counted and incubated in fresh cell culture medium containing IL-2 and IL-7 with peptide pool stimulation and FS118 antibodies or $LAG\text{-}3_1$/$PD\text{-}L1_2$ mAb[2] for 3 days. The supernatant was collected, and sLAG-3 was quantified by ELISA.

Soluble lymphocyte-activation gene 3 ELISA

To determine the concentration of sLAG-3 shed from T cells or PBMCs in the in-vitro assays, the noncompetitive antihuman LAG-3 antibody [clone 17B4; Enzo Life Sciences, Exeter, UK, ALX-804-806PF-C100 (RRID: AB_11130673)] was diluted to 1 µg/ml in PBS and used to pre-coat 96-well flat-bottomed micro-titer plates at 4 °C overnight. Plates were washed three times with PBS-Tween 20 (0.05%) then blocked with 3% BSA (A7906-100G; Sigma) in PBS. Supernatants were added, and the plate was incubated for 2 h at RT. Plates were washed three times with PBS-Tween 20 (0.05%) before FS118 (diluted 1 µg/ml in PBS-Tween 20) was added to detect captured sLAG-3. After three washes with PBS-Tween 20 (0.05%), FS118 was detected using one of two methods: (1) a biotin-conjugated anti-FS118 antibody (F-star, Cambridge, UK) followed by 1 mg/ml horseradish peroxidase-Streptavidin (405210; BioLegend, London, UK); or (2) a goat antihuman immunoglobulin G (IgG) horseradish peroxidase-conjugated antibody (A0170-1ML; Sigma) at a concentration of 0.5 µg/ml. Plates were developed with 3,3′,5,5′-tetramethylbenzidine substrate solution (N301; Thermo Fisher Scientific), and the reaction was stopped by adding 50 µl of 1 N H_2SO_4. Absorbance (450 nm) was measured using a BioTek Synergy 4 plate reader. sLAG-3 concentration was calculated by comparing unknown samples to a human LAG-3 recombinant protein (2319-L3-050; R&D Systems, Abingdon, UK) standard curve.

Mouse tumor model

All experiments were conducted under a UK Home Office Project Licence and approved by an Animal Welfare and Ethical Review Board in accordance with the UK Animal (Scientific Procedures) Act 1986 and with EU Directive EU 2010/63/EU.

The MC38 colon carcinoma cell line [Kerafast (RRID: CVCL_B288)] was initially expanded, stored, and then authenticated by short tandem repeat profiling and prescreened by IDEXX Bioresearch for pathogens using the IMPACT I protocol and shown to be pathogen free. Mycoplasma contamination was routinely monitored using the MycoProbe Mycoplasma Detection Kit (R&D Systems).

For immune-profiling studies, 8-week to 10-week-old female C57BL/6 mice [Charles River Laboratories, Tranent, UK (RRID: IMSR_JAX:000664)] were inoculated subcutaneously with 1×10^6 MC38 cells. Tumor volume (mm^3) was measured throughout the study using calipers. The following formula was used to calculate tumor volume: (length × width^2)/2. Ten days following tumor cell inoculation, all mice were divided into groups by randomization using tumor volume. Mice with tumor volumes under 13.5 mm^3 at time of randomization were excluded from the study. Twelve days following tumor cell inoculation, when tumors reached a volume of approximately 65 mm^3, each mouse received test antibodies (IgG control, FS118m, mLAG-3_1/PD-$L1_2$ mAb^2, mLAG-3/PD-1 mAb^2, or mPD-L1/LAG-3 mAb^2) via a single 200 µl intraperitoneal injection. Mice were sacrificed (96 h post-dosing), and blood and tumors collected, processed, and analyzed by flow cytometry. Mice displaying clinical observations not attributable to drug treatment were excluded from the study (one tumor ulceration and one limb wound). To minimize bias, investigators conducting observations and tumor measurements, and those performing tissue harvest and processing, were blinded to the group assignments through the study.

Flow cytometry

Mouse tumor cells were harvested, placed into GentleMACs C-tubes, and digested with the Mouse Tumor Dissociation Kit (130-096-730; Miltenyi Biotec) using the GentleMACs dissociator with Octo Heaters, according to manufacturer's instructions. Samples were filtered through a 70 µM filter, centrifuged (500*g*, 5 min) and lyzed with a 1× red blood cell lysis solution (130-094-183; Miltenyi Biotec) for 10 min at RT. Samples were centrifuged (500*g*, 5 min) again and counted on the ViCell XR; they were then centrifuged (500*g*, 5 min) and resuspended in Dulbecco's phosphate buffered saline (DPBS), ready for plating.

Blood was drawn via cardiac bleed under CO_2. The samples were plated (50 µl/well), lyzed three times with 1× red blood cell lysis solution (130-094-183; Miltenyi Biotec), and washed with DPBS.

Cells were washed in DPBS. Live/dead staining was carried out with fixable viability dye (65-0865-14; 1 : 1000 dilution in DPBS; eBioscience, Paisley, UK) for 20 min at RT. Cells were then washed twice in fluorescence-activated cell sorting (FACS) buffer (PBS/0.5% BSA/0.1% sodium azide) and blocked with human TruStain FcX (422301; BioLegend) or anti-mouse CD16/32 (14-0161-86; eBioscience) for 10 min at RT. To detect extracellular proteins, cells were labeled with fluorophore-conjugated antibodies for 45 min at 4 °C. The anti-LAG-3 antibody (clone EPR20294-9) was conjugated to fluorescein isothiocyanate (FITC) using the Lightning-Link kit (ab102884; Abcam, Cambridge, UK). Each antibody had been previously titrated to determine the optimal concentration for flow cytometry. For intracellular proteins, cell permeabilization was carried out using intracellular fixation and permeabilization buffer (00-5523-00; eBioscience) following the manufacturer's protocol, and the cells were incubated with fluorophore-conjugated antibodies overnight at 4 °C. Antibodies against the following proteins were used: CD45 [eBioscience (RRID: AB_891454)], CD3e [BioLegend (RRID: AB_2565879)], LAG-3, CD4 [BD Bioscience, Wokingham, UK (RRID: AB_2734761)], CD8 [BD Bioscience (RRID: AB_2870090)], ADAM10 [R&D Systems (RRID: AB_2242307)], inducible T-cell costimulator (ICOS) [BioLegend (RRID: AB_2122582)], and Ki67 [eBioscience (RRID: AB_11220070)] (Supplementary Table 1, Supplemental digital content 1, *http://links.lww.com/ACD/A585*). Cells were then resuspended in FACS buffer (PBS/0.5% BSA/0.1% sodium azide) for flow cytometry analysis on a Fortessa II (BD Bioscience). Analysis was performed using FlowJo software [version 10, Becton Dickinson (RRID: SCR_008520)].

The mouse LAG-3 antibody [clone C9B7W, 125208; BioLegend (RRID: AB_2133343)] has previously been shown to be noncompetitive with FS118m and detected total LAG-3 (free and bound) cell surface receptor [23]. We have also observed that the mouse LAG-3 antibody (clone EPR20294-96, ab228411; Abcam) was noncompetitive with the anti-LAG-3 Fab domains of the mPD-L1/LAG-3 mAb^2 molecule, as well as the mLAG-3 Fcab binding site of FS118m (data not shown). The C9B7W-PE antibody was used to detect total LAG-3 on murine TILs *ex vivo* following in-vivo dosing with the mLAG-3_1/PD-$L1_2$ or mLAG-3/PD-1 antibodies, compared to FS118m. The FITC-conjugated EPR20294-96 clone was used to detect total LAG-3 on murine TILs *ex vivo* following dosing with the mPD-L1/LAG-3 antibody compared to FS118m. Samples were analyzed on a Fortessa II (BD Bioscience) flow cytometer. FlowJo software was used to quantify the frequency of parent percentages of each sample. Prism software [version 10, GraphPad, Boston, Massachusetts, USA (RRID: SCR_002798)] was used to

Fig. 1

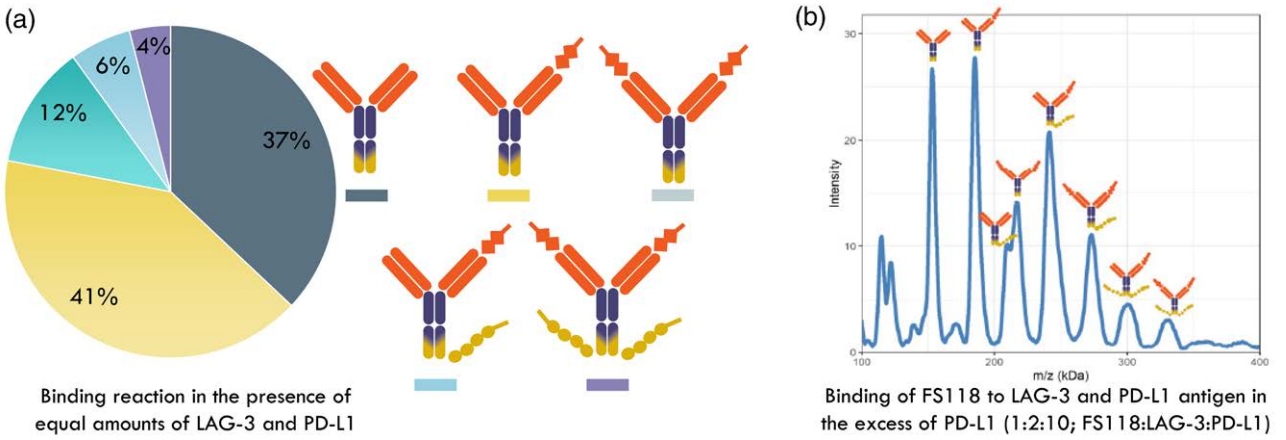

Tetravalent binding by FS118 was demonstrated using chemically crosslinked mass spectrometry mapping (XL/MS). (a) The proportion of bound and unbound FS118 in the presence of LAG-3 and PD-L1 (1 : 2 : 2 ratio). (b) An example plot showing resultant products from XL/MS of FS118 binding to LAG-3 and PD-L1 antigen in the presence of excess PD-L1 (1 : 2 : 10 ratio). LAG-3, lymphocyte-activation gene 3; PD-L1, programmed death ligand 1.

plot the measured parent % for each specific population of interest. In the flow cytometry analysis, a threshold was applied to exclude any samples with <100 events to reduce the potential for statistical bias and enhance the reliability and validity of the data.

Binding association assays

The affinity of FS118 and LAG-3_1/PD-$L1_2$ mAb² for recombinant human LAG-3 and PD-L1, and the associated binding kinetics, were assessed by surface plasmon resonance using a Biacore T200 Instrument (GE Healthcare). LAG-3 (71147; BPS Bioscience, San Diego, California, USA) or PD-L1 (AVI9049-050; R&D Systems) recombinant proteins (1 µg/ml) were injected onto Series S Sensor Chip CAP (28-9202-34; GE Healthcare) and captured using immobilized Biotin CAPture reagent (28-9202-34; GE Healthcare). Various concentrations of FS118 or LAG-3_1/PD-$L1_2$ mAb² were flowed across the chips. A 1 : 1 Langmuir model was used to generate equilibrium-binding constants (kD). Data were analyzed using Biacore T200 evaluation software v3.2 (Biacore, Cytiva).

DO11.10 T cells (National Jewish Health, Denver, Colorado, USA) engineered to overexpress murine LAG-3 or PD-1 (DO11.10.mLAG-3 or DO11.10.mPD-1, respectively) and LK35.2 B cells (ATCC, Teddington, UK) engineered to overexpress murine PD-L1 (LK35.2.mPD-L1, as described previously [23]) were incubated with serial dilutions of FS118m, mLAG-3_1/PD-$L1_2$ mAb², mLAG-3/PD-1 mAb², or IgG_1 control antibodies. The cells were washed in 1% BSA-PBS, and bound antibody was detected using an antihuman Alexa Fluor 488-conjugated secondary antibody [109-546-098-JIR-0.75 mg; Jackson Immuno Research, Ely, UK (RRID: AB_2337850)]. The samples were analyzed on a Fortessa II (BD Bioscience) flow cytometer. FlowJo software was used to quantify the mean fluorescence intensity of each sample. Prism software was used to plot the measured mean fluorescence intensity as a function of antibody concentration.

Data availability

All data used and analyzed in the current study are available from the corresponding author upon reasonable request.

Results

Validating the bispecific target binding capability of FS118

We used XL/MS to determine whether FS118 was able to bind tetravalently to LAG-3 and PD-L1. All four binding sites of FS118 were able to bind to their respective targets (LAG-3 or PD-L1) simultaneously in the presence of equal amounts of each target (Fig. 1a), as well as in the presence of excess PD-L1 (Fig. 1b).

FS118 induced shedding of cell surface lymphocyte-activation gene 3 in a manner dependent on cleavage by the metalloproteases ADAM10 and ADAM17

In primary SEB-activated human $CD4^+$ T-cell assays, FS118 induced a higher degree of LAG-3 shedding than any of the antibody controls, including an equimolar combination of component antibodies (LAG-3/mock mAb² plus PD-L1 mAb), as evidenced by levels of sLAG-3 in the supernatant (Fig. 2a). This finding was consistent across four independent individuals. To determine whether FS118-mediated LAG-3 shedding was dependent upon metalloproteases ADAM10 or ADAM17, inhibitors of these metalloproteases were added in the presence of FS118. Inhibition of ADAM10

Fig. 2

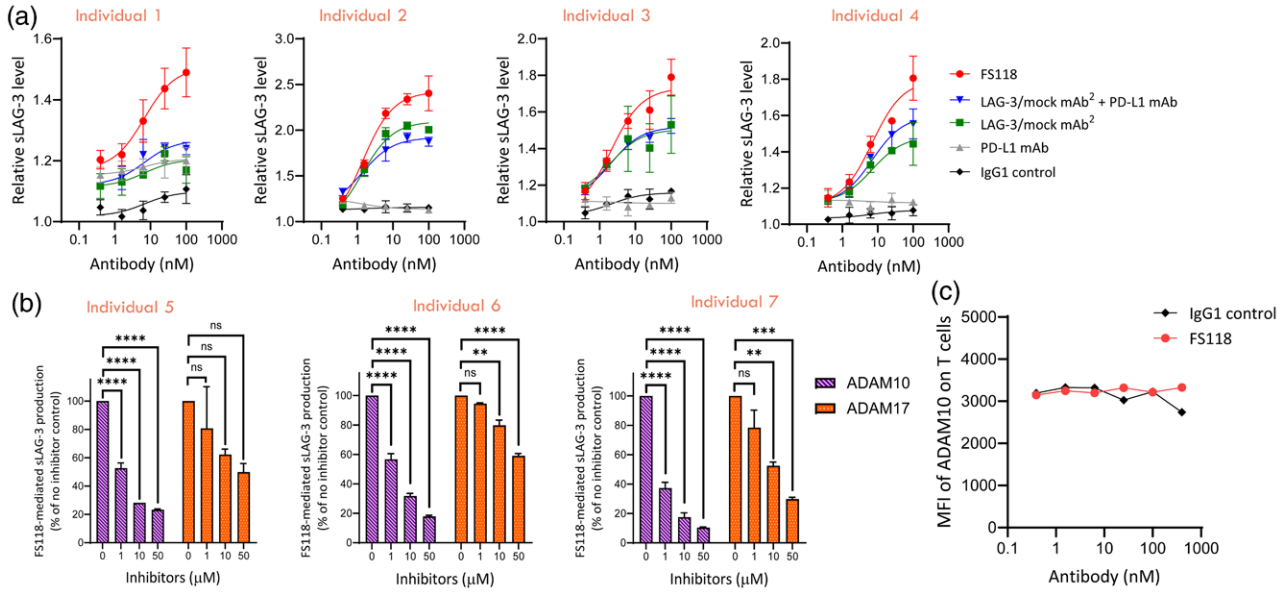

FS118-associated shedding of cell surface LAG-3 is dependent on bispecific targeting of LAG-3 and PD-L1 and mediated by metalloproteases ADAM10 and ADAM17. (a) Relative sLAG-3 levels in human SEB assays consisting of allogenic expanded CD4+ T cells and immature dendritic cells cocultured for 4 days, in response to either IgG control, FS118, anti-PD-L1 mAb, anti-LAG-3 mAb^2 mock, or the combination. Fold-changes in sLAG-3 level in the supernatant are shown. Representative graphs from four individuals of assays performed in technical triplicate. Data shown as mean ± SD. (b) LAG-3 shedding mediated by FS118 (50 nM) in SEB assays is dependent on metalloproteases ADAM10 and ADAM17. Representative graphs from four individuals of assays performed in technical duplicate. Data shown as mean ± SD. (c) Quantification of ADAM10 expression on CD4+ T cells from SEB assays with increasing concentrations of FS118 or IgG_1 control via flow cytometry. Significance determined by one-way ANOVA test. $^{**}P < 0.01$; $^{***}P < 0.001$; $^{****}P < 0.0001$; ns, not significant. IgG, immunoglobulin G; LAG-3, lymphocyte-activation gene 3; MFI, mean fluorescence intensity; PD-L1, programmed death ligand 1; SEB, Staphylococcal enterotoxin B; sLAG-3, soluble LAG-3.

or ADAM17 was associated with a dose-dependent reduction in FS118-induced LAG-3 shedding (Fig. 2b). This finding did not appear to be due to changes in metalloprotease expression, as FS118 did not impact ADAM10 expression levels on T cells in this in-vitro assay (Fig. 2c; Supplementary Fig. 1a, Supplemental digital content 1, *http://links.lww.com/ACD/A585*), or in mice bearing subcutaneous MC38 tumors (Supplementary Fig. 1b and c, Supplemental digital content 1, *http://links.lww.com/ACD/A585*).

Bivalent lymphocyte-activation gene 3 binding by FS118 is required for maximal lymphocyte-activation gene 3 shedding

To understand how the structure of FS118 mediates LAG-3 shedding, a valency variant of FS118, with monovalent LAG-3 binding in the Fcab region, was generated (LAG-3_1/PD-$L1_2$ mAb^2; Fig. 3a). In primary SEB-activated human T-cell assays, FS118 induced higher levels of sLAG-3 than the monovalent LAG-3 binding variant across three independent individuals (Fig. 3b). Similar findings were observed in antigen recall assays that used MHC class I-restricted and MHC class II-restricted stimulation (Fig. 3c). The difference in sLAG-3 levels could be due to the monovalent LAG-3 antibody (LAG-3_1/PD-$L1_2$ mAb^2) demonstrating a quicker 'off-rate' from LAG-3 than FS118, which has bivalent LAG-3 binding (Supplementary Fig. 2a, Supplemental digital content 1, *http://links.lww.com/ACD/A585*), meaning that the LAG-3_1/PD-$L1_2$ molecule more rapidly dissociates from cell surface LAG-3 before it is able to induce LAG-3 shedding. As expected, the two antibodies demonstrated similar PD-L1 binding kinetics (Supplementary Fig. 2b, Supplemental digital content 1, *http://links.lww.com/ACD/A585*).

In vivo, FS118m reduces cell surface lymphocyte-activation gene 3 on tumor-infiltrating lymphocytes and limits compensatory upregulation of lymphocyte-activation gene 3 in the periphery

To further understand the role of FS118 bivalent LAG-3 binding on LAG-3 shedding *in vivo*, murine surrogates of FS118 and LAG-3_1/PD-$L1_2$ mAb^2 were generated (FS118m and mLAG-3_1/PD-$L1_2$ mAb^2, respectively; Fig. 4a) for evaluation in a subcutaneous MC38 tumor model. Both antibodies were confirmed to bind to cells overexpressing murine LAG-3 and PD-L1 (Supplementary Fig. 3a and b, Supplemental digital content 1, *http://links.lww.com/ACD/A585*).

FS118m, with bivalent LAG-3 binding, significantly reduced the proportion of CD4+ and CD8+ TILs expressing high levels of cell surface LAG-3 (LAG-3^{hi}) relative to the IgG control (Fig. 4b; Supplementary Fig. 4a,

Fig. 3

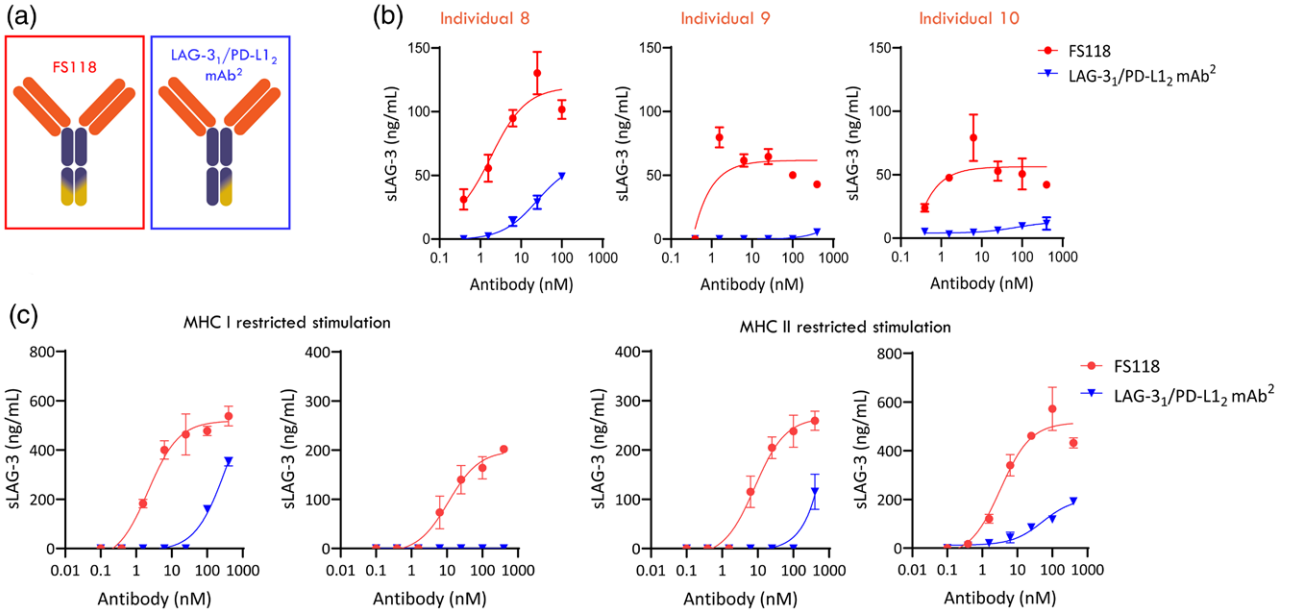

Bivalent LAG-3 binding by FS118 is required for maximal LAG-3 shedding in both CD4$^+$ and CD8$^+$ T cells. (a) A biologically similar antibody was generated, which was monovalent for LAG-3 (LAG-3$_1$) and bivalent for PD-L1 (PD-L1$_2$). Schematic representations of FS118 and LAG-3$_1$/PD-L1$_2$ mAb^2 are shown. Orange, PD-L1-binding regions; blue, fragment crystallizable region; yellow, LAG-3-binding regions. (b) The sLAG-3 level from human SEB assays consisting of allogenic expanded CD4$^+$ T cells and immature dendritic cells cocultured for 4 days, in response to either FS118 or LAG-3$_1$/PD-L1$_2$ mAb^2. sLAG-3 levels in the supernatant are shown from three individuals. Assays performed in technical duplicate, and data shown as mean ± SD. (c) MHC I- or MHC II-restricted antigen recall assay. PBMCs were stimulated with MHC I- or MHC II-restricted peptides then exposed to FS118 or LAG-3$_1$/PD-L1$_2$ mAb^2. The supernatant was collected, and sLAG-3 levels were measured by ELISA (data from two individual donors are shown). Assays performed in technical duplicate, and data shown as mean ± SD. LAG-3, lymphocyte-activation gene 3; MHC, major histocompatibility complex; PBMCs, peripheral blood mononuclear cells; PD-L1, programmed death ligand 1; SEB, Staphylococcal enterotoxin B; sLAG-3, soluble LAG-3.

Supplemental digital content 1, *http://links.lww.com/ACD/A585*). Such reductions were less notable with the mLAG-3$_1$/PD-L1$_2$ mAb^2, which were only significant for CD8$^+$ T cells (Fig. 4b).

PD-L1 blockade can lead to compensatory upregulation of other immune checkpoint proteins, such as LAG-3, in peripheral immune cells. Although this was seen with the mLAG-3$_1$/PD-L1$_2$ mAb^2, which significantly increased the proportion of CD4$^+$ and CD8$^+$ T cells in the blood expressing high levels of surface LAG-3 vs controls, FS118m demonstrated limited upregulation of LAG-3^{hi} levels (Fig. 4c; Supplementary Fig. 4b, Supplemental digital content 1, *http://links.lww.com/ACD/A585*). Consistent with this finding, FS118m was associated with a significant increase in the proportion of peripheral CD4$^+$ and CD8$^+$ T cells expressing the proliferation marker Ki67 vs control, whereas mLAG-3$_1$/PD-L1$_2$ did not induce an increase in Ki67$^+$ CD4$^+$ and CD8$^+$ T cells (Fig. 4d; Supplementary Fig. 4c, Supplemental digital content 1, *http://links.lww.com/ACD/A585*).

Analysis of the LAG-3$^-$ CD4$^+$ and CD8$^+$ T cell populations demonstrated similar findings, where a trend toward an increase in the proportion of peripheral LAG-3$^-$ CD4$^+$ and CD8$^+$ T cells expressing Ki67 (Supplementary Fig. 5a, Supplemental Digital Content 1, *http://links.lww.com/ACD/A585*) and ICOS (Supplementary Fig. 5b, Supplemental Digital Content 1, *http://links.lww.com/ACD/A585*) was observed with FS118m; the proportions of cells expressing Ki67 or ICOS were significantly higher in mice treated with FS118m than in mice treated with mLAG-3$_1$/PD-L1$_2$ mAb^2.

PD-L1, not PD-1, binding drives the reduction of surface lymphocyte-activation gene 3 on tumor-infiltrating lymphocytes and increases peripheral T-cell proliferation

To further investigate the role of the FS118m PD-L1 binding sites in modulating immune cells *in vivo*, a variant of FS118m was generated in which the PD-L1 binding sites were replaced with PD-1 binding sites (mLAG-3/PD-1 mAb^2; Fig. 5a). This mAb^2 was confirmed to bind to cells overexpressing murine LAG-3 and PD-1, but not murine PD-L1 (Supplementary Fig. 3a–c, Supplemental digital content 1, *http://links.lww.com/ACD/A585*).

In tumor-bearing mice, FS118m significantly reduced the proportion of CD4$^+$ and CD8$^+$ TILs expressing high levels of surface LAG-3 relative to the IgG control (Fig. 5b; Supplementary Fig. 4a, Supplemental digital content 1,

Fig. 4

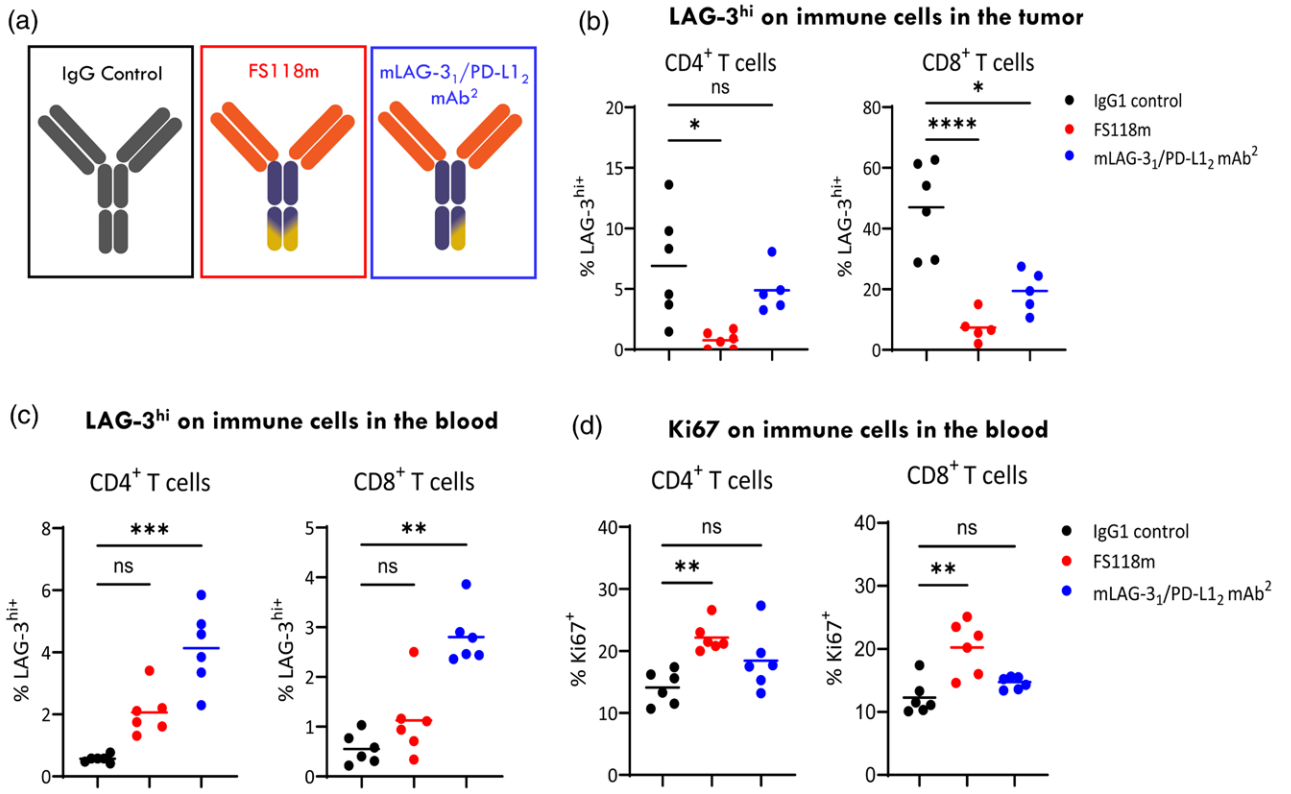

Bivalent LAG-3 binding by FS118m is required for maximal cell surface LAG-3 reduction on TILs and is associated with limited compensatory upregulation of LAG-3 in the periphery. Mice bearing subcutaneous MC38 tumors received a single intraperitoneal dose (10 mg/kg) of test antibodies. Blood and tumors were collected 96-h post dosing and analyzed by flow cytometry. (a) Murine FS118 (FS118m) and murine LAG-3$_1$/PD-L1$_2$ (mLAG-3$_1$/PD-L1$_2$ mAb^2) antibodies were generated. Schematic representations of IgG control, FS118m, and mLAG-3$_1$/PD-L1$_2$ antibodies are shown. Gray, IgG control; orange, PD-L1-binding regions; blue, fragment crystallizable region; yellow, LAG-3-binding regions. (b) Detection of LAG-3^{hi} CD4$^+$ and CD8$^+$ T cells in the tumor. (c) Detection of LAG-3^{hi} CD4$^+$ and CD8$^+$ T cells in the blood. (d) Detection of Ki67$^+$ CD4$^+$ and CD8$^+$ T cells in the blood. Significance determined by Kruskal–Wallis test. *$P < 0.05$; **$P < 0.01$; ***$P < 0.001$; ****$P < 0.0001$; ns, not significant. IgG, immunoglobulin G; LAG-3, lymphocyte-activation gene 3; PD-L1, programmed death ligand 1; TILs, tumor-infiltrating lymphocytes.

http://links.lww.com/ACD/A585). However, no significant effect on LAG-3^{hi} expression was seen with the mLAG-3/PD-1 mAb^2 (Fig. 5b).

Unlike FS118m, the mLAG-3/PD-1 mAb^2 was associated with a significant increase in peripheral CD4$^+$ and CD8$^+$ T cells expressing high levels of surface LAG-3 (Fig. 5c), and no notable increase in proliferation marker, Ki67, on these cell populations compared with FS118m and the control antibody (Fig. 5d). The mLAG-3/PD-1 mAb^2 was also not associated with an increase in the proportion of peripheral LAG-3$^-$ CD4$^+$ and CD8$^+$ T cells expressing Ki67 or ICOS (Supplementary Fig. 6a and b, Supplemental digital content 1, *http://links.lww.com/ACD/A585*), which was observed with FS118m.

Reversing the positions of the PD-L1 and LAG-3 binding sites in FS118m resulted in less effective reduction of surface LAG-3 in tumor-infiltrating lymphocytes

A reverse orientation antibody was generated in which the positions of the PD-L1 and LAG-3 binding sites of FS118m were reversed (mPD-L1/LAG-3 mAb^2; Fig. 6a). The mPD-L1/LAG-3 mAb^2 was confirmed to bind to cells expressing murine LAG-3 and PD-L1 (Supplementary Fig. 3d and e, Supplemental digital content 1, *http://links.lww.com/ACD/A585*). In tumor bearing mice, the mPD-L1/LAG-3 mAb^2 did not reduce the proportion of CD4$^+$ or CD8$^+$ TILs expressing high levels of LAG-3 when compared with FS118m. Additionally, the mPD-L1/LAG-3 mAb^2 did not significantly reduce LAG-3 expression vs control in either cell type (Fig. 6b).

Discussion

Here we demonstrate that the tetravalent, bispecific features of FS118 are key to its unique mechanism of action. Substituting or removing individual binding domains of FS118, or the murine surrogate FS118m, resulted in impaired cleavage of LAG-3 from TILs, compensatory upregulation of high LAG-3 expression on peripheral immune cells, and reduced proliferation of peripheral immune cells.

Fig. 5

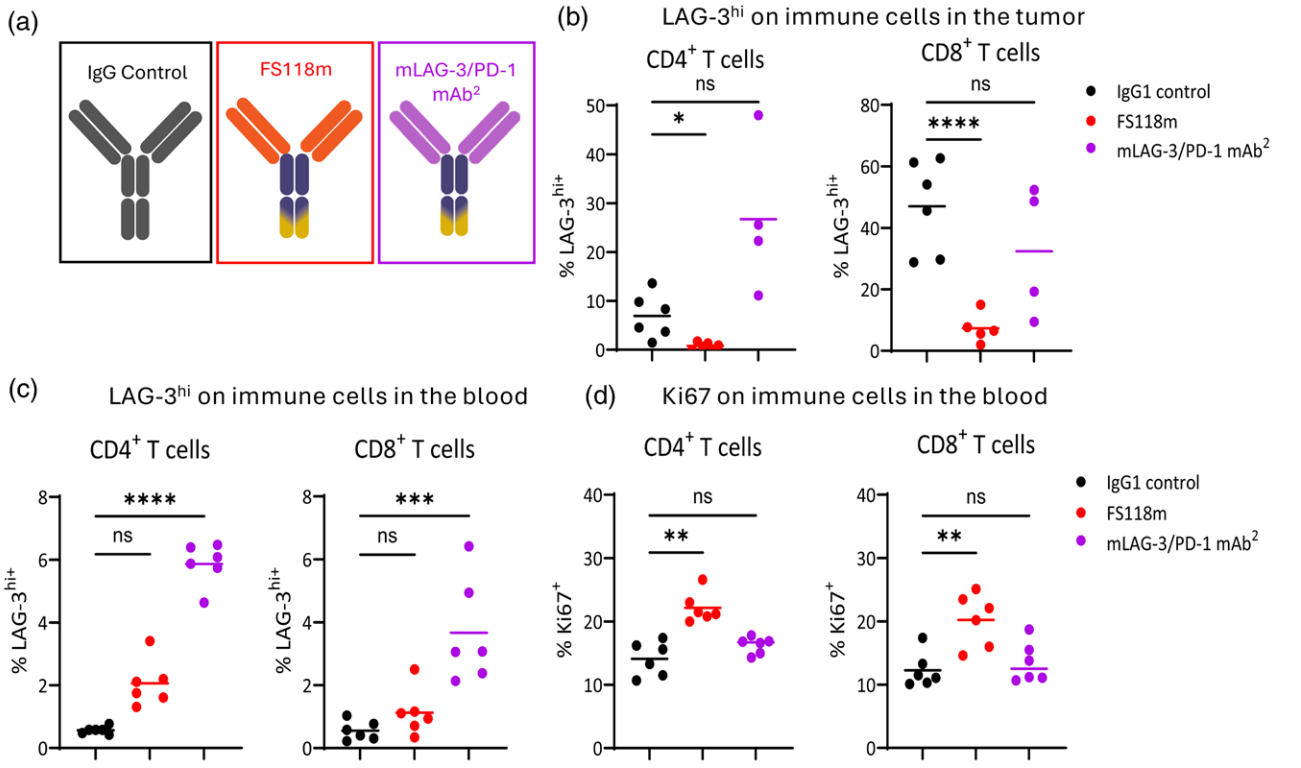

Reduction of cell surface LAG-3 on TILs, and increased proliferation of peripheral effector cells, was driven by binding to PD-L1 but not PD-1. Mice bearing subcutaneous MC38 tumors received a single intraperitoneal dose (10 mg/kg) of test antibodies. Blood and tumors were collected 96-h post dosing and analyzed by flow cytometry. (a) A murine antibody was generated which was bivalent for both LAG-3 and PD-1 (mLAG-3/PD-1). Schematic representations of IgG control, FS118m, and mLAG-3/PD-1 antibodies are shown. Gray, IgG control; orange, PD-L1-binding regions; blue, fragment crystallizable region; yellow, LAG-3-binding regions; purple, PD-1 binding regions. (b) Detection of LAG-3^{hi} CD4^{+} and CD8^{+} T cells in the tumor. (c) Detection of LAG-3^{hi} CD4^{+} and CD8^{+} T cells in the blood. (d) Detection of Ki67^{+} CD4^{+} and CD8^{+} T cells in the blood. Significance determined by Kruskal–Wallis test. *$P < 0.05$; **$P < 0.01$; ***$P < 0.001$; ****$P < 0.0001$; ns, not significant. IgG, immunoglobulin G; LAG-3, lymphocyte-activation gene 3; PD-1, programmed cell death 1; PD-L1, programmed death ligand 1; TILs, tumor-infiltrating lymphocytes.

Being structurally homologous to CD4, the ability of LAG-3 to recognize MHC class II-peptide complexes and inhibit CD4^{+} T cells has been well described [31,32]. Although LAG-3 has also been shown to suppress CD8^{+} T cells to a degree [when antigen-presenting cells (APCs) express both MHC class I and MHC class II-peptide complexes], the mechanisms for this are less clear [32]. Our data show that FS118 and FS118m induce shedding of LAG-3 from both CD4^{+} and CD8^{+} T cells which, in turn, may induce proliferation of these cells. Interestingly, LAG-3 has previously been shown to inhibit CD4^{+} and CD8^{+} T-cell function in the absence of MHC class II, demonstrating that LAG-3 can function in an MHC class II-independent manner; LAG-3-deficient T cells were shown to have higher effector function *in vitro* and an increased ability to expand *in vivo* [33,34]. These findings indirectly support our own data, where the absence of LAG-3 through FS118m-mediated shedding resulted in an increase in CD8^{+} T-cell responses. These data highlight that LAG-3 should not only be thought of in the context of classical CD4 biology, but also in the context of CD8^{+} T-cell activation. This is important given that responses to immune checkpoint inhibitors have been correlated with both CD4^{+} and CD8^{+} T-cell immunity [35–37].

In our study, FS118-mediated shedding of LAG-3 was driven by metalloproteases ADAM10 and ADAM17. To our knowledge, this is the first time that this has been shown for any LAG-3/PD-(L)1 bispecific antibody. ADAM10 and ADAM17 are important cell surface metalloproteases known to mediate LAG-3 cleavage [38,39], a process that is required for normal T-cell activation and proliferation [38]. In mice, when metalloprotease-mediated shedding of LAG-3 from T cells was absent due to expression of a non-cleavable LAG-3, the T cells were resistant to PD-1 blockade and could not effectively mount antitumor responses [25]. Consistent with these findings, in a cohort of patients with advanced skin cancer, patients with disease progression on standard-of-care anti-PD-1/CTLA-4 immunotherapy had significantly higher LAG-3 expression on CD4^{+} conventional T cells than patients who did respond [25]. Furthermore,

Fig. 6

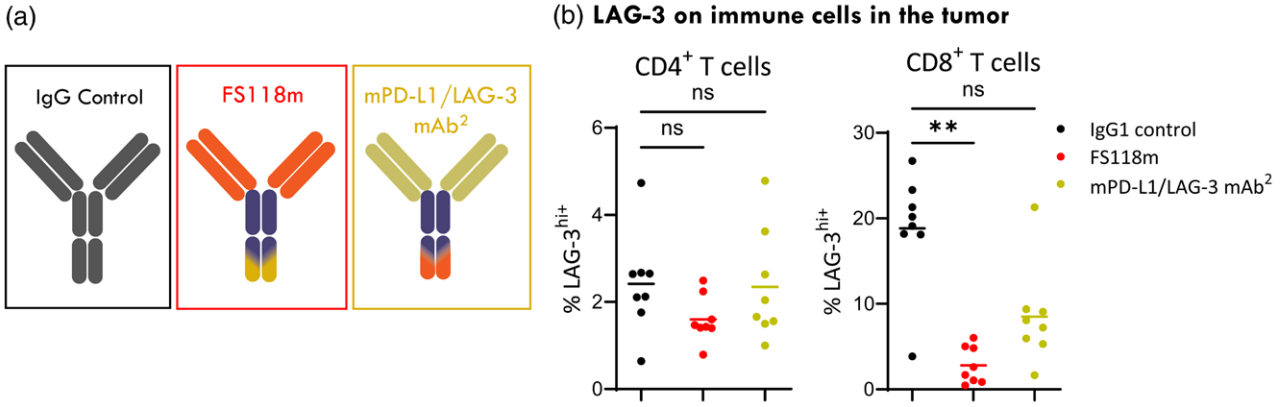

Reduction of cell surface LAG-3 on TILs following exposure to FS118m or a 'reverse orientation' antibody in which the LAG-3 and PD-L1 binding sites were reversed. (a) Schematic representations of IgG control, FS118m, and reverse orientation mPD-L1/LAG-3 antibodies are shown. Gray, IgG control; orange, PD-L1-binding regions; blue, fragment crystallizable region; yellow, LAG-3-binding regions. (b) Mice bearing subcutaneous MC38 tumors received a single intraperitoneal dose (10 mg/kg) of test antibodies. Blood and tumors were collected 96 h post dosing and analyzed by flow cytometry to detect LAG-3^{hi} CD4$^+$ and CD8$^+$ T cells in the tumor. Significance determined by Kruskal–Wallis test. $^{**}P < 0.01$; ns, not significant. LAG-3, lymphocyte-activation gene 3; PD-L1, programmed death ligand 1; TILs, tumor-infiltrating lymphocytes.

the ratio of LAG-3 to ADAM10 in CD4$^+$ conventional T cells was significantly higher in patients who progressed on treatment compared with those who responded, suggesting that LAG-3 may be a key mechanism of resistance to immunotherapy [25]. Given FS118 targets both LAG-3 and PD-L1, it may have a potential benefit in patients with high LAG-3 expression, who may otherwise not respond to anti-PD-L1 monotherapy. We found that FS118 was associated with a greater degree of ADAM10/ADAM17-mediated LAG-3 shedding than antibodies monovalent for LAG-3. Similarly, the greatest reduction in cell surface LAG-3 expression on exhausted TILs, defined as T cells expressing high levels of LAG-3, was observed with FS118m compared with a mAb^2 in which the positions of the PD-L1 and LAG-3 binding sites were reversed. One hypothesis to explain these findings is that the LAG-3 bivalency in the fragment crystallizable region of FS118 allows clustering of LAG-3, which optimizes cleavage by ADAM10/ADAM17 and thus shedding. FS118 may also preferentially bind to dimeric LAG-3 receptors, which are associated with the TCR/CD3 complex and required for optimal inhibitory function of LAG-3 [40]. By contrast, a single LAG-3 binding site in the fragment crystallizable region, or two LAG-3 binding sites spatially separated on the Fab regions, were less efficient at inducing shedding, potentially because clustering of LAG-3 could not occur as effectively when FS118 bound to LAG-3 monomers. Whether sLAG-3 has a function is yet to be determined [41,42], although early in-vitro studies using a sLAG-3-immunoglobin fusion protein suggested it may play a role in activating T cells via binding to MHC class II receptors on APCs [43,44].

Our data comparing FS118m with a variant antibody in which the PD-L1 binding sites were replaced with PD-1 binding sites indicate that crosslinking LAG-3 (on T cells) to PD-L1 (on APCs/tumor cells), rather than to PD-1 (on T cells), was better at removing high levels of LAG-3 from exhausted T cells and increasing effector-cell proliferation. Whether this translates to additional antitumor benefit over a LAG-3/PD-1 mAb^2 is unclear, because both FS118m [23] and a LAG-3/PD-1 co-targeting multi-specific Humabody (CB213) [45] have inhibited tumor growth in syngeneic mouse models. However, the importance of LAG-3 shedding in overcoming resistance to anti-PD-1 immunotherapy has been suggested in a recent preclinical study [25].

Preclinical studies have demonstrated compensatory upregulation of LAG-3 in TILs in response to PD-1 blockade [9,10]. In our study, compensatory upregulation of LAG-3 to high levels on peripheral immune cells was limited by the dual LAG-3/PD-L1 blockade of FS118, but not by the antibody monovalent for LAG-3 or the surrogate antibody with LAG-3/PD-1 binding, indicating the importance of the tetravalency and LAG-3/PD-L1 bispecificity of FS118. Indeed, in a study using peripheral blood from healthy volunteers, there was no noticeable difference in compensatory upregulation of LAG-3 in invariant natural killer T cells following dual blockade with anti-LAG-3 and anti-PD-1 antibodies vs anti-PD-1 alone [46]. Thus, dual blockade of LAG-3 and PD-L1 may be more effective at limiting compensatory upregulation of LAG-3 than dual blockade of LAG-3 and PD-1. The potential clinical importance of limiting such upregulation is highlighted by the fact that a LAG-3$^+$ immunotype in peripheral blood has been shown to correlate with poor outcomes following anti-PD-1 or anti-CTLA-4 treatment in patients with urothelial carcinoma or melanoma [47].

Available mouse models may lack the sensitivity to easily assess the effects of combining LAG-3 and PD-(L)1 blockade on antitumor efficacy. While FS118m has demonstrated significantly greater tumor growth inhibition vs an anti-PD-L1 antibody [23], several other studies have not shown significant differences in antitumor efficacy between dual blockade of LAG-3/PD-(L)1 and PD-(L)1 alone [48–50]. We speculate that most models used to evaluate LAG-3/PD-(L)1 blockade are very sensitive to PD-(L)1 blockade, and thus there is only a small window in which to show additive/synergistic effects with the combination. As such, cellular systems, such as those described here, are important to help understand how a mAb^2 works, as they can better assess the impact of changes to format/structure. The application of this approach can also be applied to other targets where bivalency is important.

Overall, our data demonstrate the importance of the structure and valency of the bispecific antibody FS118 in eliciting biological effects. FS118 was well-tolerated in the Phase I portion [21] of a Phase I/II trial in patients with advanced solid tumors that had progressed on prior anti-PD-(L)1 therapy (NCT03440437). In the Phase II stage of the trial, the antitumor efficacy and safety of FS118 (as monotherapy or in combination with paclitaxel) was investigated in patients with squamous cell carcinoma of the head and neck with acquired resistance to PD-(L)1 inhibition.

Acknowledgements

The authors thank F-star and invoX colleagues, particularly the Protein Sciences and in-vivo Teams, for their technical contributions, useful discussions on the data, and review of the manuscript. Dr Chris Guise and Victoria Lord of Bioscript Group, Cheshire, UK, provided medical writing assistance (funded by F-star).

Conflicts of interest

All authors were employees of F-star Therapeutics at the time their work was performed. There are no conflicts of interest.

References

1 McLane LM, Abdel-Hakeem MS, Wherry EJ. CD8 T cell exhaustion during chronic viral infection and cancer. *Annu Rev Immunol* 2019; **37**:457–495.
2 He X, Xu C. Immune checkpoint signaling and cancer immunotherapy. *Cell Res* 2020; **30**:660–669.
3 Francisco LM, Sage PT, Sharpe AH. The PD-1 pathway in tolerance and autoimmunity. *Immunol Rev* 2010; **236**:219–242.
4 Joller N, Kuchroo VK. Tim-3, Lag-3, and TIGIT. *Curr Top Microbiol Immunol* 2017; **410**:127–156.
5 Han Y, Liu D, Li L. PD-1/PD-L1 pathway: current researches in cancer. *Am J Cancer Res* 2020; **10**:727–742.
6 Chang E, Pelosof L, Lemery S, Gong Y, Goldberg KB, Farrell AT, *et al.* Systematic review of PD-1/PD-L1 inhibitors in oncology: from personalized medicine to public health. *Oncologist* 2021; **26**:e1786–e1799.
7 Sharma P, Hu-Lieskovan S, Wargo JA, Ribas A. Primary, adaptive, and acquired resistance to cancer immunotherapy. *Cell* 2017; **168**:707–723.
8 Pathak R, Pharaon RR, Mohanty A, Villaflor VM, Salgia R, Massarelli E. Acquired resistance to PD-1/PD-L1 blockade in lung cancer: mechanisms and patterns of failure. *Cancers (Basel)* 2020; **12**:3851.
9 Koyama S, Akbay EA, Li YY, Herter-Sprie GS, Buczkowski KA, Richards WG, *et al.* Adaptive resistance to therapeutic PD-1 blockade is associated with upregulation of alternative immune checkpoints. *Nat Commun* 2016; **7**:10501.
10 Huang RY, Francois A, McGray AR, Miliotto A, Odunsi K. Compensatory upregulation of PD-1, LAG-3, and CTLA-4 limits the efficacy of single-agent checkpoint blockade in metastatic ovarian cancer. *Oncoimmunology* 2017; **6**:e1249561.
11 Grosso JF, Kelleher CC, Harris TJ, Maris CH, Hipkiss EL, De Marzo A, *et al.* LAG-3 regulates CD8+ T cell accumulation and effector function in murine self- and tumor-tolerance systems. *J Clin Invest* 2007; **117**:3383–3392.
12 Chocarro L, Blanco E, Zuazo M, Arasanz H, Bocanegra A, Fernandez-Rubio L, *et al.* Understanding LAG-3 signaling. *Int J Mol Sci* 2021; **22**:5282.
13 Sega EI, Leveson-Gower DB, Florek M, Schneidawind D, Luong RH, Negrin RS. Role of lymphocyte activation gene-3 (LAG-3) in conventional and regulatory T cell function in allogeneic transplantation. *PLoS One* 2014; **9**:e86551.
14 Triebel F, Jitsukawa S, Baixeras E, Roman-Roman S, Genevee C, Viegas-Pequignot E, Hercend T. LAG-3, a novel lymphocyte activation gene closely related to CD4. *J Exp Med* 1990; **171**:1393–1405.
15 Chocarro L, Blanco E, Arasanz H, Fernandez-Rubio L, Bocanegra A, Echaide M, *et al.* Clinical landscape of LAG-3-targeted therapy. *Immunooncol Technol* 2022; **14**:100079.
16 OPDUALAG prescribing information. https://www.accessdata.fda.gov/drugsatfda_docs/label/2024/761234s006lbl.pdf. Last updated March 2024. [Accessed 03 February 2025]
17 OPDUALAG summary of product characteristics. https://www.ema.europa.eu/en/medicines/human/EPAR/opdualag. Last updated 06 January 2025. [Accessed 03 February 2025]
18 Tawbi HA, Schadendorf D, Lipson EJ, Ascierto PA, Matamala L, Castillo Gutierrez E, *et al.* Relatlimab and nivolumab versus nivolumab in untreated advanced melanoma. *N Engl J Med* 2022; **386**:24–34.
19 Hamid O, Lewis KD, Weise A, McKean M, Papadopoulos KP, Crown J, *et al.* Phase I study of fianlimab, a human lymphocyte activation gene-3 (LAG-3) monoclonal antibody, in combination with cemiplimab in advanced melanoma. *J Clin Oncol* 2024; **42**:2928–2938.
20 Lin CC, Garralda E, Schoffski P, Hong DS, Siu LL, Martin M, *et al.* A phase 2, multicenter, open-label study of anti-LAG-3 ieramilimab in combination with anti-PD-1 spartalizumab in patients with advanced solid malignancies. *Oncoimmunology* 2024; **13**:2290787.
21 Yap TA, LoRusso PM, Wong DJ, Hu-Lieskovan S, Papadopoulos KP, Holz JB, *et al.* A phase 1 first-in-human study of FS118, a tetravalent bispecific antibody targeting LAG-3 and PD-L1 in patients with advanced cancer and PD-L1 resistance. *Clin Cancer Res* 2023; **29**:888–898.
22 Everett KL, Kraman M, Wollerton FPG, Zimarino C, Kmiecik K, Gaspar M, *et al.* Generation of Fcabs targeting human and murine LAG-3 as building blocks for novel bispecific antibody therapeutics. *Methods* 2019; **154**:60–69.
23 Kraman M, Faroudi M, Allen NL, Kmiecik K, Gliddon D, Seal C, *et al.* FS118, a bispecific antibody targeting LAG-3 and PD-L1, enhances T-cell activation resulting in potent antitumor activity. *Clin Cancer Res* 2020; **26**:3333–3344.
24 Arduin E, Arora S, Bamert PR, Kuiper T, Popp S, Geisse S, *et al.* Highly reduced binding to high and low affinity mouse Fc gamma receptors by L234A/L235A and N297A Fc mutations engineered into mouse IgG2a. *Mol Immunol* 2015; **63**:456–463.
25 Andrews LP, Somasundaram A, Moskovitz JM, Szymczak-Workman AL, Liu C, Cillo AR, *et al.* Resistance to PD1 blockade in the absence of metalloprotease-mediated LAG3 shedding. *Sci Immunol* 2020; **5**:eabc2728.
26 Atwell S, Ridgway JB, Wells JA, Carter P. Stable heterodimers from remodeling the domain interface of a homodimer using a phage display library. *J Mol Biol* 1997; **270**:26–35.
27 Wines BD, Powell MS, Parren PW, Barnes N, Hogarth PM. The IgG Fc contains distinct Fc receptor (FcR) binding sites: the leukocyte receptors Fc gamma RI and Fc gamma RIIa bind to a region in the Fc distinct from that recognized by neonatal FcR and protein A. *J Immunol* 2000; **164**:5313–5318.
28 Bich C, Maedler S, Chiesa K, DeGiacomo F, Bogliotti N, Zenobi R. Reactivity and applications of new amine reactive cross-linkers for mass spectrometric detection of protein-protein complexes. *Anal Chem* 2010; **82**:172–179.
29 Smith TM Jr, Tharakan A, Martin RK. Targeting ADAM10 in cancer and autoimmunity. *Front Immunol* 2020; **11**:499.
30 Bai H, Zhang L, Sun P, Wu H, Li M, Gu Y, *et al.* ADAM17: a novel treatment target for aneurysms. *Biomed Pharmacother* 2022; **148**:112712.

31 Maruhashi T, Okazaki IM, Sugiura D, Takahashi S, Maeda TK, Shimizu K, Okazaki T. LAG-3 inhibits the activation of CD4+ T cells that recognize stable pMHCII through its conformation-dependent recognition of pMHCII. *Nat Immunol* 2018; **19**:1415–1426.

32 Maruhashi T, Sugiura D, Okazaki IM, Okazaki T. LAG-3: from molecular functions to clinical applications. *J ImmunoTher Cancer* 2020; **8**:e001014.

33 Workman CJ, Vignali DA. The CD4-related molecule, LAG-3 (CD223), regulates the expansion of activated T cells. *Eur J Immunol* 2003; **33**:970–979.

34 Workman CJ, Vignali DA. Negative regulation of T cell homeostasis by lymphocyte activation gene-3 (CD223). *J Immunol* 2005; **174**:688–695.

35 Dolina JS, Van Braeckel-Budimir N, Thomas GD, Salek-Ardakani S. CD8+ T cell exhaustion in cancer. *Front Immunol* 2021; **12**:715234.

36 Oh DY, Kwek SS, Raju SS, Li T, McCarthy E, Chow E, *et al*. Intratumoral CD4+ T cells mediate anti-tumor cytotoxicity in human bladder cancer. *Cell* 2020; **181**:1612–1625.e13.

37 Kagamu H, Kitano S, Yamaguchi O, Yoshimura K, Horimoto K, Kitazawa M, *et al*. CD4+ T-cell immunity in the peripheral blood correlates with response to anti-PD-1 therapy. *Cancer Immunol Res* 2020; **8**:334–344.

38 Li N, Wang Y, Forbes K, Vignali KM, Heale BS, Saftig P, *et al*. Metalloproteases regulate T-cell proliferation and effector function via LAG-3. *EMBO J* 2007; **26**:494–504.

39 Morisaki Y, Ohshima M, Suzuki H, Misawa H. LAG-3 expression in microglia regulated by IFN-gamma/STAT1 pathway and metalloproteases. *Front Cell Neurosci* 2023; **17**:1308972.

40 Adam K, Lipatova Z, Abdul Ghafoor Raja M, Mishra AK, Mariuzza RA, Workman CJ, Vignali DAA. Cutting edge: LAG3 dimerization is required for TCR/CD3 interaction and inhibition of antitumor immunity. *J Immunol* 2024; **213**:7–13.

41 Burnell SEA, Capitani L, MacLachlan BJ, Mason GH, Gallimore AM, Godkin A. Seven mysteries of LAG-3: a multi-faceted immune receptor of increasing complexity. *Immunother Adv* 2022; **2**:ltab025.

42 Graydon CG, Mohideen S, Fowke KR. LAG3's enigmatic mechanism of action. *Front Immunol* 2020; **11**:615317.

43 Avice MN, Sarfati M, Triebel F, Delespesse G, Demeure CE. Lymphocyte activation gene-3, a MHC class II ligand expressed on activated T cells, stimulates TNF-alpha and IL-12 production by monocytes and dendritic cells. *J Immunol* 1999; **162**:2748–2753.

44 Casati C, Camisaschi C, Rini F, Arienti F, Rivoltini L, Triebel F, *et al*. Soluble human LAG-3 molecule amplifies the in vitro generation of type 1 tumor-specific immunity. *Cancer Res* 2006; **66**:4450–4460.

45 Edwards CJ, Sette A, Cox C, Di Fiore B, Wyre C, Sydoruk D, *et al*. The multi-specific V_H-based Humabody CB213 co-targets PD1 and LAG3 on T cells to promote anti-tumour activity. *Br J Cancer* 2022; **126**:1168–1177.

46 Balasko AL, Kowatsch MM, Graydon C, Lajoie J, Fowke KR. The effect of blocking immune checkpoints LAG-3 and PD-1 on human invariant Natural Killer T cell function. *Sci Rep* 2023; **13**:10082.

47 Shen R, Postow MA, Adamow M, Arora A, Hannum M, Maher C, *et al*. LAG-3 expression on peripheral blood cells identifies patients with poorer outcomes after immune checkpoint blockade. *Sci Transl Med* 2021; **13**:eabf5107.

48 Jiang H, Ni H, Zhang P, Guo X, Wu M, Shen H, *et al*. PD-L1/LAG-3 bispecific antibody enhances tumor-specific immunity. *Oncoimmunology* 2021; **10**:1943180.

49 Marcq E, Van Audenaerde JRM, De Waele J, Merlin C, Pauwels P, van Meerbeeck JP, *et al*. The search for an interesting partner to combine with PD-L1 blockade in mesothelioma: focus on TIM-3 and LAG-3. *Cancers (Basel)* 2021; **13**:282.

50 Burova E, Hermann A, Dai J, Ullman E, Halasz G, Potocky T, *et al*. Preclinical development of the anti-LAG-3 antibody REGN3767: characterization and activity in combination with the anti-PD-1 antibody cemiplimab in human PD-1xLAG-3-knockin mice. *Mol Cancer Ther* 2019; **18**:2051–2062.